



Article

Analysis of AVAZ Seismic Forward Modeling of Fracture-Cavity Reservoirs of the Dengying Formation, Central Sichuan Basin

Yisheng Liu ¹, Zhengping Zhu ^{1,*}, Renfang Pan ¹, Bole Gao ² and Jineng Jin ¹

¹ School of Geoscience, Yangtze University, Wuhan 430100, China; lys06372@163.com (Y.L.); pan@yangtzeu.edu.cn (R.P.); jjn@yangtzeu.edu.cn (J.J.)

² Southwest Petroleum Bureau of China Petrochemical Corporation, Chengdu 610000, China; gaobole@foxmail.com

* Correspondence: zhuzhengping199908@163.com; Tel.: +86-18627091297

Abstract: For the purpose of clarifying the seismic response characteristics of fractured-cavity reservoirs of Dengying Formation in the central Sichuan Basin, the paper first intends to establish three geological models of fracture cave reservoirs based on drilling, logging, and core data of the Dengying Formation in the central Sichuan Basin. Then, the formation reflection is calculated with reference to anisotropic Horizontal Transverse Isotropy (HTI) medium. Finally, further research on Amplitude Variation with Azimuth (AVAZ) seismic forward modeling has been conducted to clarify the seismic response characteristics of different reservoir types in the study area. The results suggest that: Seismic response characteristics of fractured-cavity reservoirs are controlled by incident angle and azimuth angle of seismic waves in different types of reservoirs. The incident angle of the seismic wave controls the difference in amplitude caused by different micro-fracture densities, and the azimuth angle controls the identification ability of the micro-fracture direction. The increase in incident angle brings about a gradual decline in amplitude. The magnitude reaches the highest when the azimuth is parallel to the normal direction of the fracture surface; however, it'll come down to the lowest as the azimuth is perpendicular to the normal direction of the fracture surface. The fracture density fails to affect the amplitude as long as the azimuth angle is parallel to the direction of the fracture. However, the decreased amplitude reflects the increasing fracture density as the azimuth angle is identical to the normal direction of the fracture surface. The comparison between the theoretical model of three different types of fractured-cavity reservoirs and the actual uphole trace shows that the model has high accuracy. The prospect of seismic identification of fractured-cavern reservoirs, based on the results, can provide us with feasible and applicable evidence for future research on seismic identification of reservoirs and prediction of fracture distribution in the Dengying Formation of central Sichuan.



Citation: Liu, Y.; Zhu, Z.; Pan, R.; Gao, B.; Jin, J. Analysis of AVAZ Seismic Forward Modeling of Fracture-Cavity Reservoirs of the Dengying Formation, Central Sichuan Basin. *Energies* **2022**, *15*, 5022. <https://doi.org/10.3390/en15145022>

Academic Editor: Mofazzal Hossain

Received: 26 May 2022

Accepted: 6 July 2022

Published: 9 July 2022

Publisher's Note: MDPI stays neutral with regard to jurisdictional claims in published maps and institutional affiliations.



Copyright: © 2022 by the authors. Licensee MDPI, Basel, Switzerland. This article is an open access article distributed under the terms and conditions of the Creative Commons Attribution (CC BY) license (<https://creativecommons.org/licenses/by/4.0/>).

Keywords: fracture-cavity reservoir; HTI medium; AVAZ; anisotropy; forward modeling

1. Introduction

In recent decades, significant breakthroughs have been made in the exploration of the carbonate fracture-cavity reservoirs of the Sinian Dengying Formation in the central Sichuan Basin. Du [1] and Yu [2] indicated that carbonate fracture-cavity reservoirs are one of the key reservoir types in Western China. Typically, researchers have in practice found that karst reservoirs are mainly distributed in the central Sichuan Basin, yet the fracture characteristics show complex and abnormally weak seismic responses because of the distinguishing features of fracture-cavity reservoirs [3], which are small in total scale and quite imbalanced in their vertical development [4], leading to the multisolution nature of seismic reservoir prediction [5,6]. Therefore, defining the influence of seismic response characteristics affected by variable reservoir space is essential for the prediction of fracture-cavity carbonate reservoirs.

The adoption of the forwarding modeling performed by predecessors in previous studies facilitates further research into the seismic response characteristics of fracture-cavity reservoirs. Ma [7] and Sun [8] made great efforts to analyze the formation mechanism of the “bead-like” reflection caused by the fracture-cave body, making a further contribution to discussions on the variation law of amplitude intensity of fracture-cave bodies. Additionally, Ma [9] and Yang [10] and Bachrach [11] probed into the influence of cave development on the seismic response characteristics of fracture-cave reservoirs, analyzing the impact of the caves on the “bead-like” reflection characteristics of fracture-cave reservoirs. Furthermore, Wang [12] and Chen [13] placed great emphasis on the variation in fluid changes in fracture-cavity reservoirs using AVO forward modeling. They discussed the reflection of the AVO response characteristics of fracture-cavity reservoirs during fluid filling, laying the basic groundwork for effectively predicting actual fracture-cavity reservoirs. Generally, the establishment of the relationship between large-scale karst caves and “beaded” reflection has become the main focus of current research on seismic forward modeling of carbonate rocks, but this does not apply to fracture-cavity reservoirs with small-scale caves and high fracture density, such as that which occurs in the Dengying Formation in central Sichuan. Bachrach [11] proposed an AVAZ inversion framework with VTI constraints based on Bayesian theory for orthorhombic media. Narhari [14] applied the orthorhombic prestack AVAZ inversion method to carbonate fractures based on the linear slip model. Seismic AVAZ inversion has also been studied and applied in shale gas fields [15,16]. Fu [17] studied the limitations of the P-wave amplitude versus azimuth (AVAZ) inversion of fracture-attribute parameters using numerical modeling. However, studies of this kind of reservoir are relatively rare at present. As significant contributors dedicated to this field, Wang [18], Xiao [19], and Weng [20], whose efforts have now been recognized, established forward models of different reservoir morphologies by analyzing the statistical petrophysical parameters of reservoirs and simulating the reservoir development morphology. They proposed that reservoir development morphology is the main factor causing changes in reservoir seismic response characteristics. Bao [21,22], Thai [23], and Thanh [24] have established fracture models to characterize the relationship between fractured reservoirs and geological and petrophysical parameters. However, in addition to the development of the reservoir itself, the processing of fractures and voids and their anisotropic features are also primary causes of shifts in the seismic response characteristics of fracture-cavity reservoirs [25–27]. Therefore, it is essential to establish a forward model serving as a critical pillar that can directly reflect the influence of fractures and voids on seismic response characteristics in fracture-cavity reservoirs.

Based on previous studies combined with generalized drilling, logging, and geological data from the study area, this paper aims to construct three types of fracture-cavity reservoir geological models. By applying anisotropic TI medium theory and using the Rüger reflection coefficient calculation formula, it helps to establish an AVAZ gathering and superimposed profile model, which successfully classifies the seismic anisotropic response characteristics of the three types of the fracture-cavity reservoir. Furthermore, the development of fractures in fracture-cavity reservoirs was set to be altered to summarize the rules of reflection characteristics brought about by fracture density in fracture-cavity reservoirs. Based on the efforts described above, our results present reliable evidence for the effective prediction of fractures and the reservoir itself. Compared with the existing research, the three kinds of fracture cave reservoir geological models designed in this study are more practical, and forward models that can directly reflect the influence of fractures and holes in fracture cave reservoir on seismic response characteristics is established, which is more suitable for fracture cave reservoir with small hole size and high fracture density in Dengying Formation in Central Sichuan.

2. Geological Background and Building Model

2.1. Geological Facts

The study area is located in the Weiyuan Longnsvi structural belt of the Middle Sichuan gentle paleo-uplift structural area, Sichuan Basin, surrounded by Suining City, Ziyang City, Anyue County, Tongnan County, and Chongqing City (Figure 1). The Dengying Formation developed from marine carbonate rock deposition, with its thick stratum present in a NE–SW direction, and the Gaoshiti block is more than 700 m thick [28]. The residual thickness, generated from the targeted fourth segment of the Dengying Formation, measures 0~400 m, characterized by continuous deposition with the third segment of the Dengying Formation. Afterward, due to the regional uplift movement of the second and third episodes of Tongwan and the erosion of strata exposed to denudation, the residual thickness developed into an unconformity contact with the Lower Cambrian Madiping Formation or the Qiongzhusi Formation of the overlying strata. The lithology of this study area is dominated by arenaceous dolomite and algal dolomite, with siliceous bands, few bacteria and algae, and stromatolites. Sizeable residual thickness is one of the features of the fourth segment of the Dengying Formation in the Gaoshiti block. Additionally, a rapid pinch-out was created by the Deyang–Anyue rift trough west of the Gaoshiti block [29].

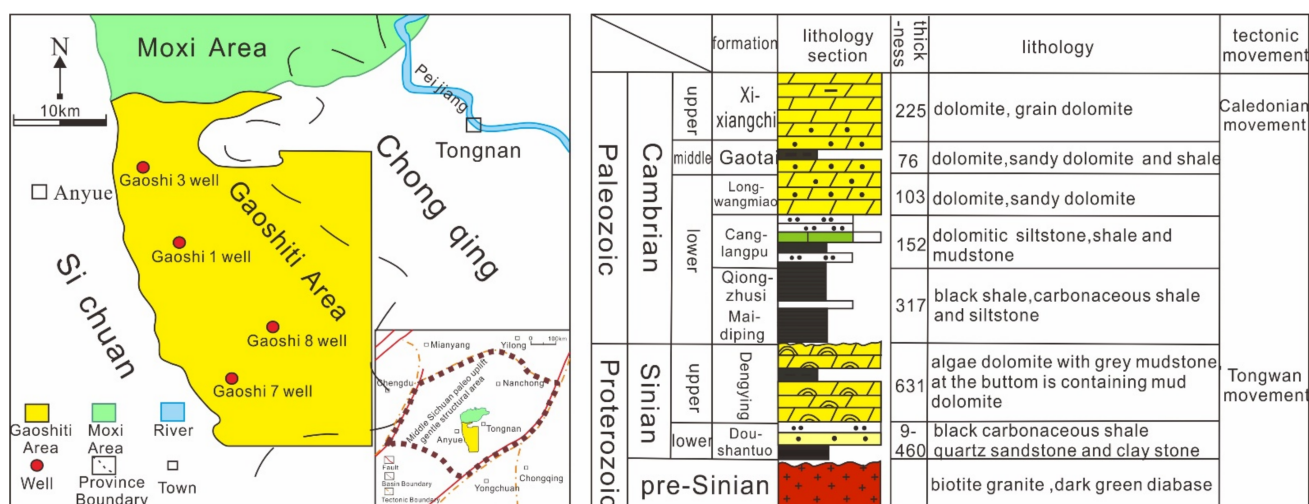


Figure 1. Location map and stratum of the study areas.

2.2. Characteristics of Reservoir Pore Space

Concerning the complex internal reservoir space of the Fourth member of the Dengying Formation in the study area, matrix pores, dissolution pores, and fractures comprise the main reservoir space. (1) The pore types of the Dengying Formation reservoir in the study area, primarily dissolution pores, are divided into three categories: intergranular dissolution, intergranular, and intragranular dissolution pores. Intergranular dissolved pores are common, of uneven shape and size, and some are filled with calcite. Intergranular pores are characterized by poor connectivity and irregular shape, whereas intergranular dissolved pores are well preserved and without filling. (2) The voids can be primarily separated into pore types and fracture types: the former are derived from pore dissolution with poor connectivity and the latter are developed partly as a result of the expansion of fractures in the epigenetic period. (3) The Dengying Formation has been affected by several tectonic episodes, namely, the Tongwan, Caledonian, Indosinian, Himalayan, and Yanshan, with an enormous number of microfractures caused by tectonic movement transformation and geological tectonic stress [30]. Among these, pores constitute the main reservoir space, whereas the fractures create the seepage channels between pores [31]. Please refer to Table 1 for the specific parameters of reservoir fractures and cavities.

Table 1. Fracture and cavity parameters of the reservoir.

		Types	Size
Pore	dissolution pores	amygdaloid inner dissolution pores	<2 mm
		dissolved dissolution pores in grains	
		dissolved dissolution pores between grains	
		intercrystal dissolution pores	
		organism pore	
Cavity		fractured cavity	>2 mm
		pore dissolved holes	<20 mm
Fracture	structural fracture	packing fracture	length 500–800 mm, width 0.2–0.5 mm, fracture number 0.3–0.5 per meter
		open fracture	
		dissolution fractures	-

2.3. Characteristics of Reservoir Vertical Combination

There are broad differences in the distribution of fractures and caves in the Fourth member of the Dengying Formation in Central Sichuan. A set of siliceous strips that are several meters thick divide it into two parts: continuously developed fractures and caves in the upper part of the siliceous reservoir and uneven horizontal development of pores and fractures in the lower part of the reservoir (Figure 2). In view of the different evolution of fractures and caves in the lower part of the siliceous strip, Xiao [19] separated the reservoirs of the Fourth member of the Dengying Formation in the study area into three types. Type I: fracture-cavity reservoir + siliceous strip + fracture-cavity reservoir (such as Gaoshi well 8); Type II: fracture-cavity reservoir + siliceous strip + cave reservoir (such as Gaoshi well 3); Type III: fracture-cavity reservoir + siliceous strip + relatively dense layer reservoir (such as Gaoshi well 103).

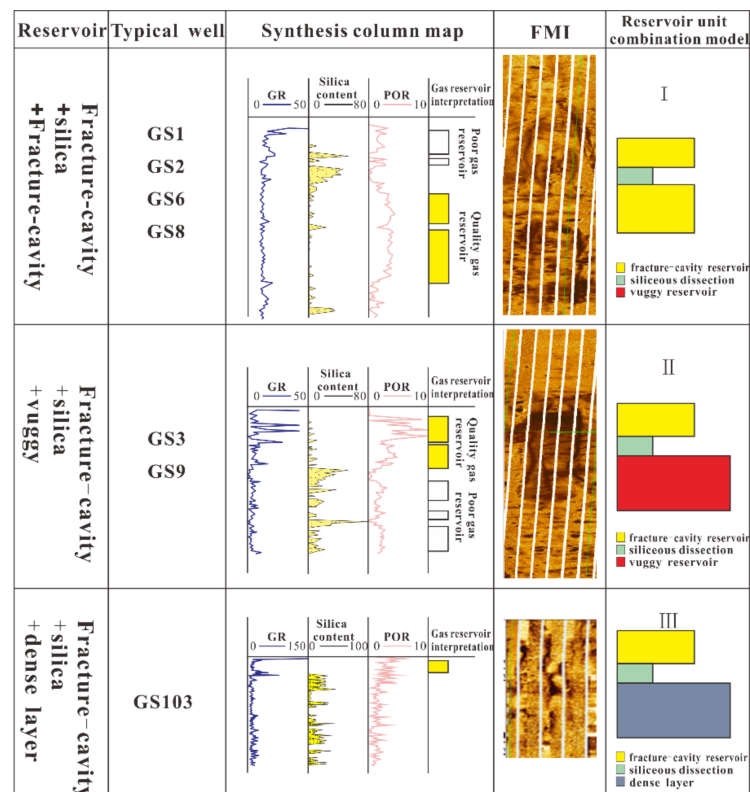


Figure 2. Well and logging data corresponding to three reservoir types in the geological model.

2.4. Construction of the Geological Model

Based on our understanding of the spatial characteristics of reservoirs and their unit combinations in the study area, we designed three typical fracture-cavity reservoir stratigraphic models for the study area (Figure 3): (1) the type I stratigraphic model has the following features: a thickness of 220 m, capped by 70 m deep mudstone of the Qiongzhusi Formation, a 30 m deep fracture-cavity reservoir in the upper reservoir, a 20 m thick siliceous interlayer, and the lower part a 40 m thick cave reservoir; (2) the type II stratigraphic model has the following features: a cumulative thickness of 220 m, the caprock is mudstone of the Qiongzhusi Formation, a thickness of 60 m, a 40 m thick upper reservoir that is a fracture-cavity reservoir, the interlayer is a 30 m thick siliceous layer, and the lower reservoir is a 30 m thick fracture cave reservoir; (3) the type III stratigraphic model has the following features: an overall thickness of 220 m, embedded with mudstone of the Qiongzhusi Formation as its caprock, which is 50 m thick, and the upper part of the reservoir comprises a 30 m deep fracture-cavity reservoir. The interlayer is characterized by a siliceous layer with a thickness of 30 m. The lower part is a relatively dense layer with a 30 m thickness. Table 2 gives the specific rock physical parameters of the model.

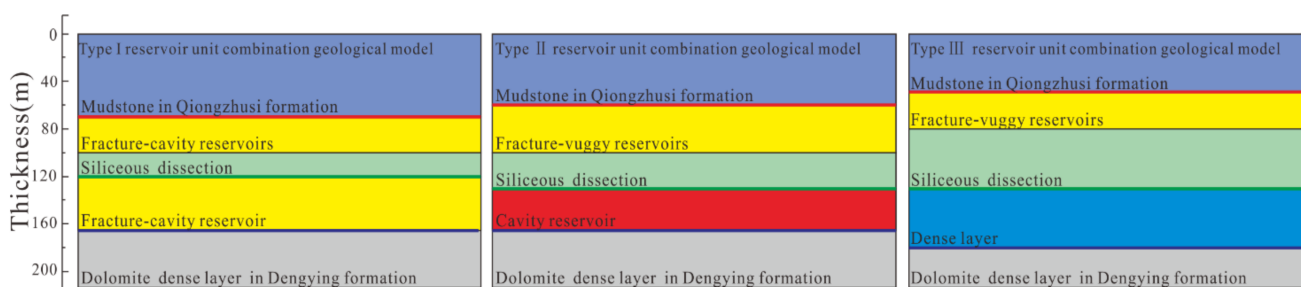


Figure 3. Three types of typical fracture-cavity reservoir stratigraphic models.

Table 2. Petrophysical parameters of the reservoirs.

Reservoir Type	Reservoir Unit	P-Wave m/s	S-Wave m/s	Density g/cm ³
I	Mudstone in Qiongzhusi Formation	4900	2841	2.57
	Fracture-cavity reservoir	6000	3510	2.7
	Siliceous dissection	6200	3624	2.72
	Fracture-cavity reservoir	6100	3567	2.71
	Dolomite dense layer in Dengying Formation	6800	3966	2.79
II	Mudstone in Qiongzhusi Formation	4900	2841	2.57
	Fracture-cavity reservoir	5700	3909	2.78
	Siliceous dissection	6200	3624	2.72
	Cavity reservoir	5800	3388	2.68
	Dolomite dense layer in Dengying Formation	6800	3966	2.79
III	Mudstone in Qiongzhusi Formation	4900	2841	2.58
	Fracture-cavity reservoir	6200	3624	2.74
	Siliceous dissection	6300	3681	2.75
	Dense layer	6600	3852	2.78
	Dolomite dense layer in Dengying Formation	6800	3966	2.80

3. Anisotropic Reflection Theory of Fracture-Cavity Reservoirs

TI media are generally used to describe anisotropic media. As the uniform layer fracture develops, it can be considered a VTI medium (Figure 4a). However, as opposed to VTI, the uniform layer medium containing the vertical fracture is termed an HTI medium (Figure 4b), and a fracture that has a certain dip angle or nonhorizontal arrangement can be called a TTI medium (Figure 4c). Concerning the relatively gentle strata in the study area, the fractures have high angle characteristics, and the pores and caves in the reservoir show

no signs of anisotropy. Therefore, at a certain level, the pores can be regarded as isotropic background parameters, and then the anisotropic reflection coefficient can be obtained as a result of using fractures by calculation in the form of anisotropy alone. The type of medium with a high-angle crack located in the physical parameters of the entire background can be regarded as an HTI medium.

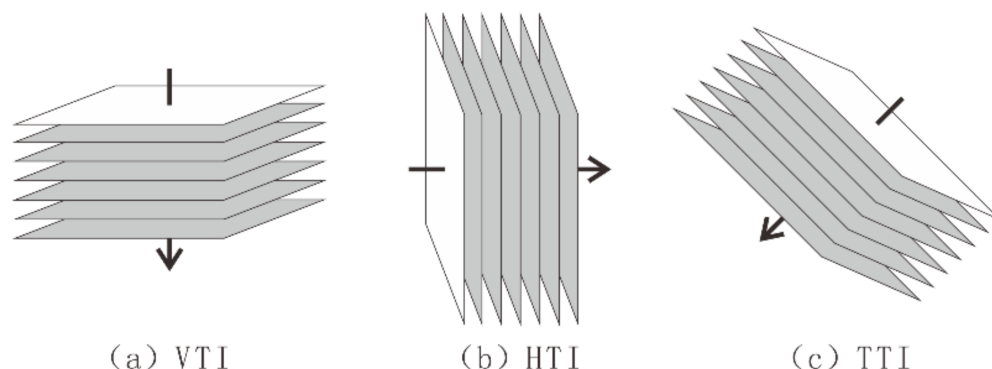


Figure 4. TI anisotropic medium.

3.1. Thomsen’s Anisotropic Parameters

To facilitate theoretical research and practical application, Thomsen proposed three anisotropic coefficients, i.e., ϵ , γ and δ , which are combinations of elastic coefficients [32–35]. Coefficient ϵ is approximately equal to the relative difference between the horizontal and vertical velocities of the P-wave, and its size reflects the anisotropy strength; coefficient γ demonstrates the anisotropy of the S-wave, and coefficient δ indicates the curvature of the P-wave phase velocity curve in the direction of symmetry [36–38].

According to Hudson’s theory, Bakunin [39] discussed the correspondence between the Thomsen parameter of HTI medium and fracture density E , considering that when the fracture contains gas:

$$\begin{aligned} \epsilon^{(V)} &\approx -\frac{8}{3}e \\ \gamma^{(V)} &\approx -\frac{8e}{3(3-2g)} \\ \delta^{(V)} &\approx -\frac{8}{3}e \left[1 + \frac{g(1-2g)}{(3-2g)(1-g)} \right] \end{aligned} \tag{1}$$

The superscript (V) works under HTI medium as Thomsen’s three parameters, and g is the velocity ratio of transverse and longitudinal waves, and e is the fracture density, dimensionless. The calculation formula of fracture density e can be written as follows:

$$e = Na^3/V \tag{2}$$

where N represents the cracks with average radius and a represents the amounts in unit volume V .

Based on these relationships, we calculated the fracture density and Thomsen parameters of the reservoir in the study area. Table 3 presents the specific calculation results.

Table 3. Thomsen’s parameters correspond to different fracture densities.

Model Type	Layer Type	Microfracture Density	$\epsilon^{(V)}$	$\gamma^{(V)}$	$\delta^{(V)}$
High fracture density	Covering strata	/	/	/	/
	Reservoir	0.053	−0.14	−0.08	−0.12
Real fracture density	Covering strata	/	/	/	/
	Reservoir	0.026	−0.07	−0.04	−0.06

Table 3. Cont.

Model Type	Layer Type	Microfracture Density	$\varepsilon^{(V)}$	$\gamma^{(V)}$	$\delta^{(V)}$
Medium fracture density	Covering strata	/	/	/	/
	Reservoir	0.013	-0.04	-0.02	-0.03
Low fracture density	Covering strata	/	/	/	/
	Reservoir	0.007	-0.02	-0.01	-0.02

The snapshot in Figure 5 presents the change rule of Thomsen anisotropic parameters for different fracture densities of the reservoir in the study area. The anisotropic parameters gradually decrease as the fracture density increases.

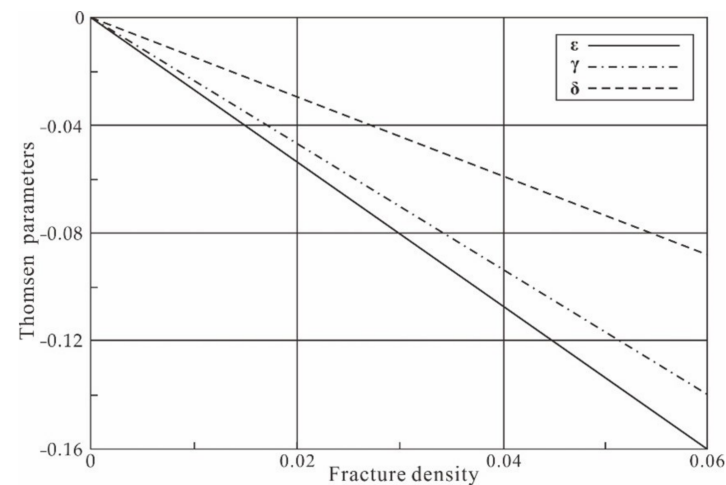


Figure 5. Thomsen's parameters and fracture density.

3.2. Reservoir Reflection Coefficient

Rüger [40] proposed an approximate formula of the P-P wave reflection coefficient in weakly anisotropic HTI media, which is based on the approximate formula of the P-P wave reflection coefficient in isotropic HTI media:

$$R_P^{sym}(\theta, \phi) = \frac{\Delta Z}{2Z} + \frac{1}{2} \left\{ \frac{\Delta \alpha}{\alpha} - \left(\frac{2\bar{\beta}}{\alpha} \right)^2 \frac{\Delta G}{G} + \left[\Delta \delta^{(V)} + 8 \left(\frac{\bar{\beta}}{\alpha} \right)^2 \Delta \gamma \right] \cos^2(\phi - \phi_{sym}) \right\} \sin^2 \theta + \left\{ \frac{\Delta \alpha}{\alpha} + \frac{1}{2} \left[\Delta \varepsilon^{(V)} \sin^2(\phi - \phi_{sym}) + \Delta \delta^{(V)} \cos^2(\phi - \phi_{sym}) \right] \sin^2(\phi - \phi_{sym}) \right\} \sin^2 \theta \tan^2 \theta \quad (3)$$

where θ is the incident angle, ϕ represents the azimuth angle, ϕ_{sym} is the symmetrical axis direction (the normal direction of the fracture surface), α is the longitudinal wave velocity of the isotropic surface of HTI medium, β is the SH wave velocity of all isotropic surfaces of the HTI medium, Z is the longitudinal wave impedance, G is the shear modulus, α and β are the mean values of the upper and lower layer parameters, and Δ is the parameter difference between the upper and lower layers.

The Rüger formula enables us to apply the measured physical property parameters of the study area to the calculation, under different fracture densities, of the weak anisotropic reflection coefficient, which is selected from three different types of fracture-cavity reservoir characterized by varying angles of incident and azimuth angles. The detailed research process is shown in Figure 6.

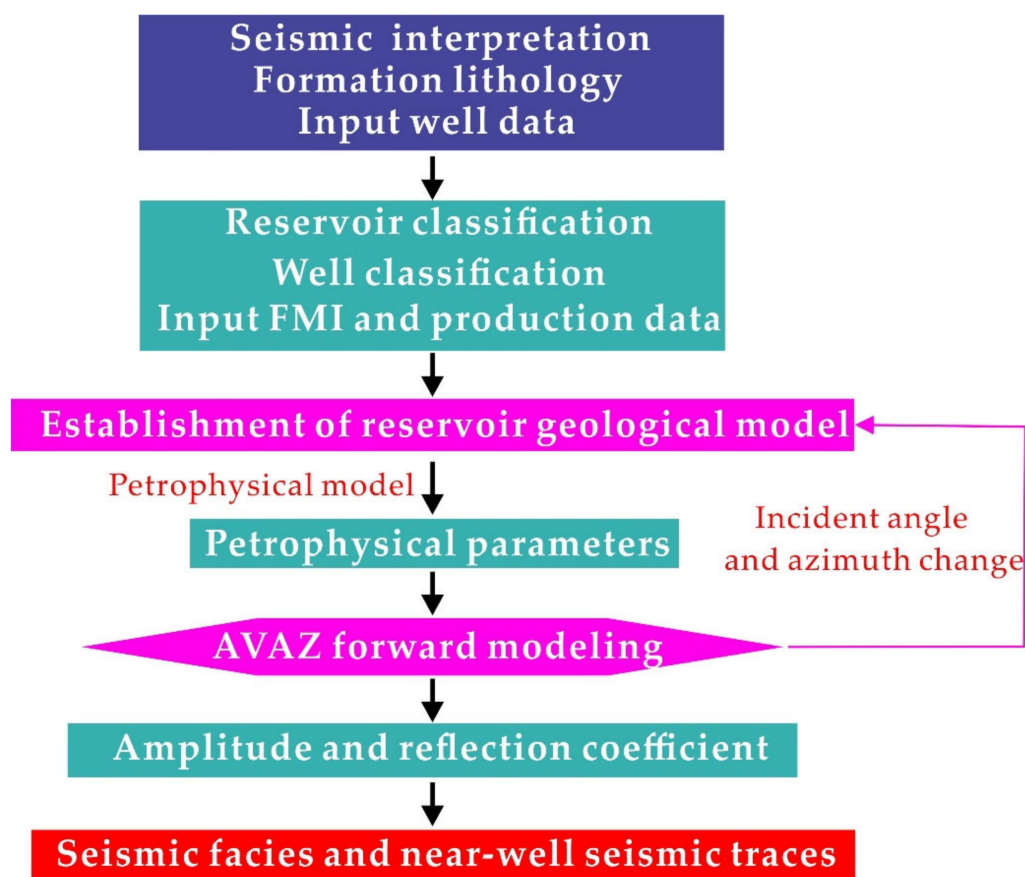


Figure 6. AVAZ reflection coefficient of the model.

The specific change rule of the reflection coefficient is shown in Figure 7. The results, as shown in the figure, present the azimuth angles of 0° and 180° as fracture strike, and a certain similarity exists in the reflection coefficient changes for the three reservoir types. In general, the characteristics of the top interface of the reservoir show a positive reflection. With the same incident angle, the reflection coefficient of the fracture cavity reservoir increases as fracture density surges, and it is symmetrical along the fracture symmetry axis (i.e., azimuth 90° and 270°). However, the reflection coefficient of the fracture-cavity reservoir decreases as the incident angle declines. When the azimuth approaches the average direction of the fracture surface (i.e., 90° and 270°), the reflection coefficient gradually reaches its lowest level until it is parallel to the average direction of the fracture surface. In light of this, based on the AVAZ characteristics, an analysis of the fracture trend of the reservoir in the study could be conducted to indicate the change in fracture density, which is reflected to a certain extent by the reflection coefficient.

Combined with the calculation results of the anisotropic reflection coefficient of the three categories of the fracture–cavity reservoir, this forward modeling used the 40 Hz primary frequency Reiko subwave to conduct convolution calculations for three types of geological models with different reservoir combinations, obtaining three types of AVAZ channel collection models (Figure 8). In the figure, the transverse arrangement is a manifestation of different fracture densities and the longitudinal method exhibits different reservoir types.

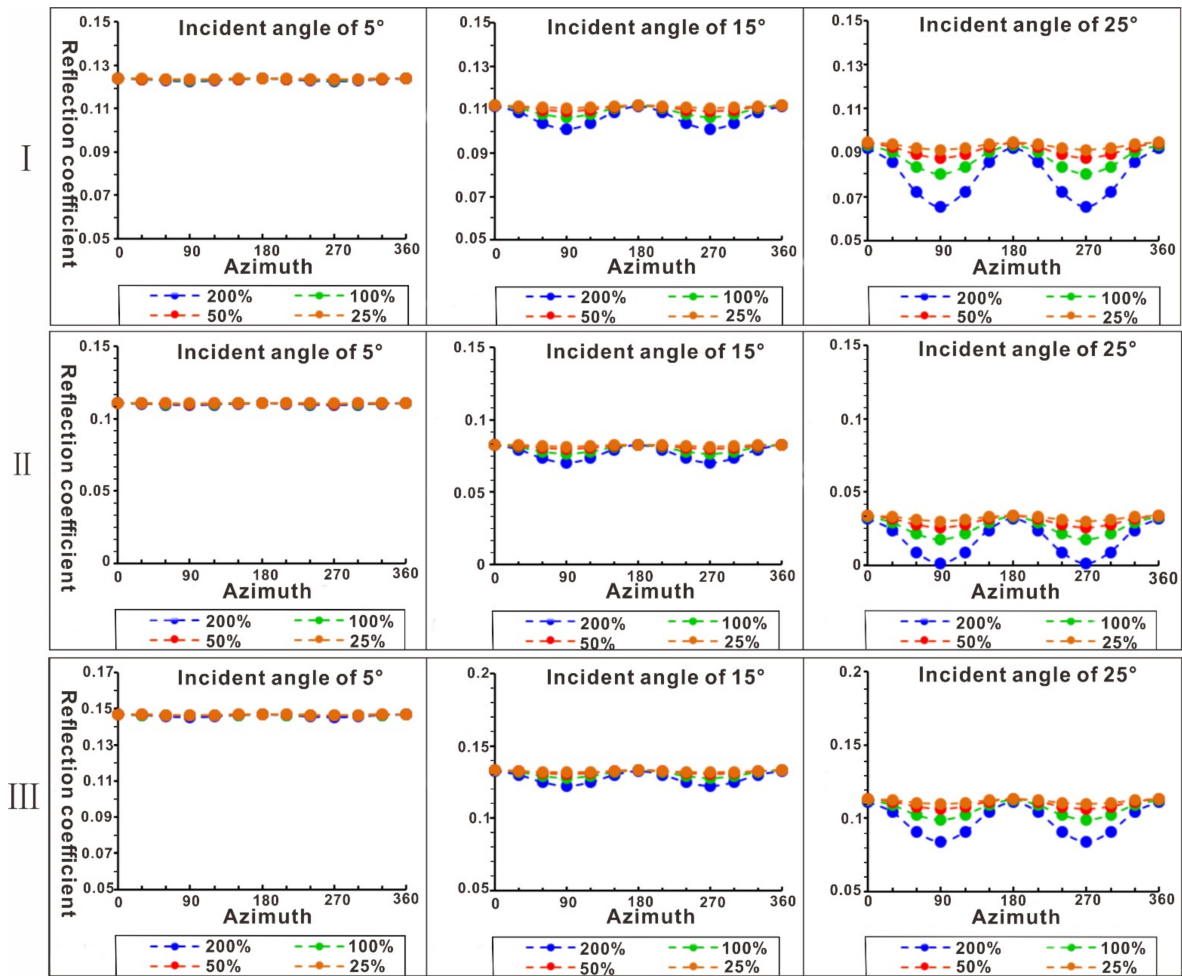


Figure 7. AVAZ reflection coefficient of the model. **I:** fracture-cavity reservoir + siliceous strip + fracture-cavity reservoir. **II:** fracture-cavity reservoir + siliceous strip + cave type reservoir. **III:** fracture-cavity reservoir + siliceous strip + relatively dense layer. 4. AVAZ Forward Modeling and Its Analysis.

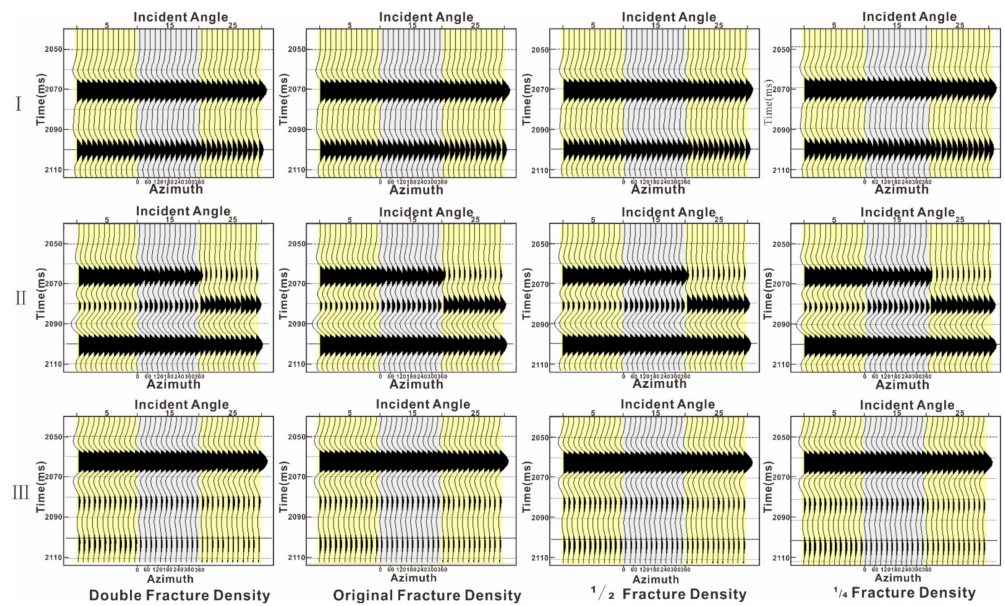


Figure 8. AVAZ gather forward model. **I:** fracture-cavity reservoir + siliceous strip + fracture-cavity

reservoir. **II**: fracture-cavity reservoir + siliceous strip + cave type reservoir. **III**: fracture-cavity reservoir + siliceous strip + relatively dense layer.

4. Summary and Discussion

4.1. Characteristics of Seismic Response

There is a huge difference in the wave characteristics of the AVAZ gathers in the three types of reservoirs (Figure 9). The AVAZ gathers of the type I reservoir are characterized by “wide troughs”. The amplitude of the top and bottom interfaces of the reservoir declines gradually as the incident angle increases with the slowly increasing amplitude of the internal trough of the reservoir. The AVAZ gathers of the type II reservoir present the characteristic of “wide troughs + highlights”, with the amplitude of the top interface falling sharply as the incident angle rises, whereas that of the bottom interface declines slowly and the “highlights” in the reservoir increase correspondingly, with a “double highlights” feature forming after full angle superposition. The AVAZ gathers of the type III reservoir show the feature of “wide troughs + highlights” where the top interface of the reservoir shows a strong wave peak, with a weak wave peak in the bottom interface, the interior of the reservoir features the characteristic of “highlights”, and the overall amplitude intensity of the reservoir is in accordance with the increase in incident angle. However, the trend is not apparent.

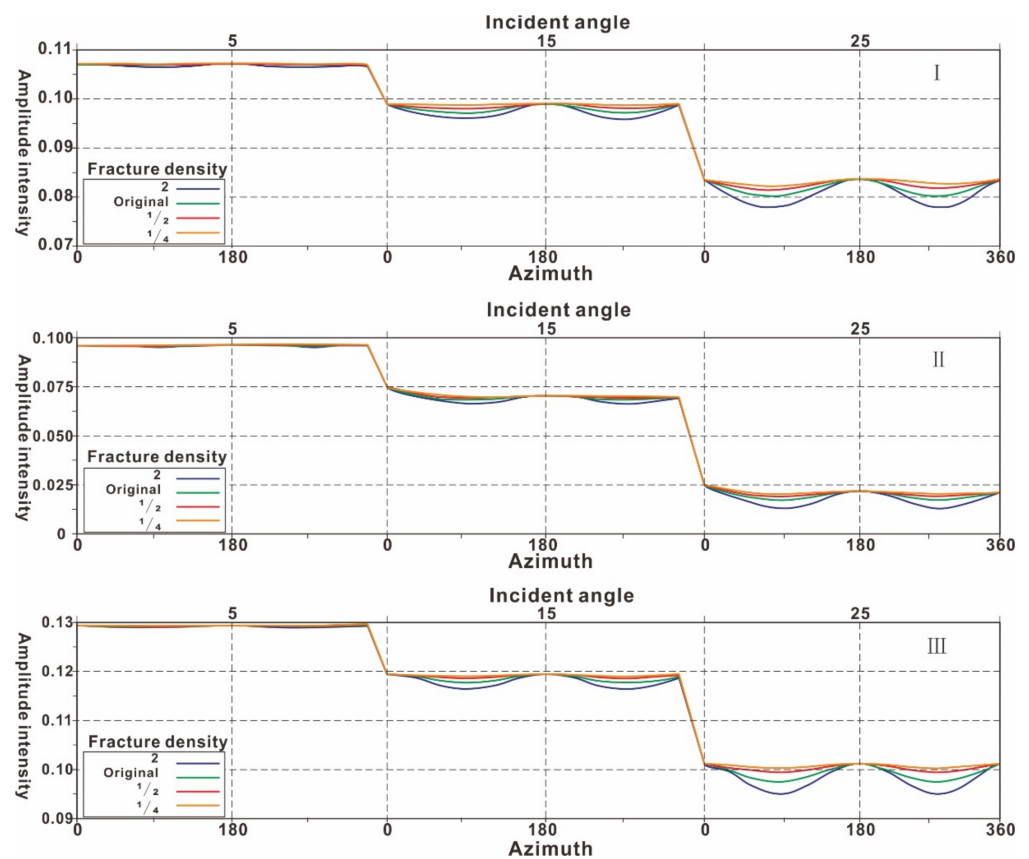


Figure 9. Amplitude attribute analysis of the AVAZ gathers. **I**: fracture-cavity reservoir + siliceous strip + fracture-cavity reservoir. **II**: fracture-cavity reservoir + siliceous strip + cave type reservoir. **III**: fracture-cavity reservoir + siliceous strip + relatively dense layer.

4.2. Characteristics of Seismic Facies

Application of a 40 Hz primary frequency Reiko subwave assisted in the calculation of the reservoir reflection coefficient at 0° azimuth by convolution and obtaining the reservoir stack profile model, which indicates the characteristics of the seismic facies of the reservoir are highly consistent with those of the measured seismic data. When the reservoir unit

combination was “fracture-cavity reservoir + siliceous layer + fracture-cavity reservoir”, i.e., the type I reservoir, the seismic facies showed “wide trough” reflection characteristics; in the case of the “fracture-cavity reservoir + siliceous layer + cave type reservoir”, i.e., the type II reservoir, the seismic facies presented “wide trough + double highlights” reflection characteristics; however, the “fracture-cavity reservoir + siliceous layer + more dense layer”, i.e., the type III reservoir, made the seismic facies exhibit the reflection characteristics of “wide trough + highlight” (Figure 10).

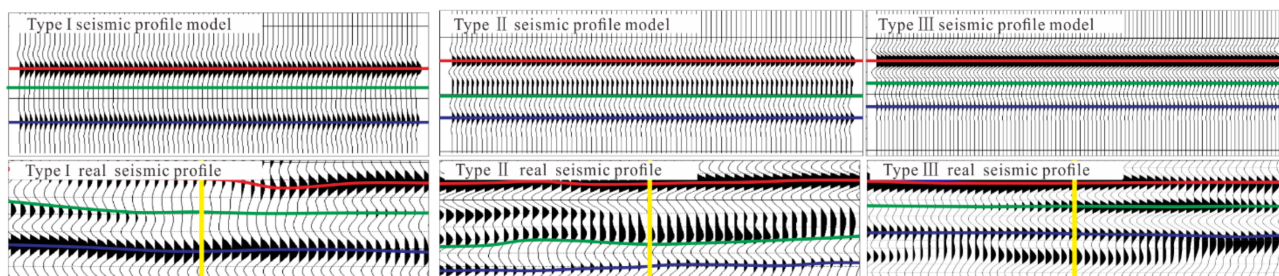


Figure 10. Comparisons of forward modeling.

The advantage of this study is that it fully considers the distribution law of reservoir lithology and designs a reasonable geological theoretical model, which can directly reflect the influence of fractures and holes in fracture cave reservoirs on seismic response characteristics, making the model more suitable for fracture cave reservoirs with small pore size and high fracture density such as Dengying Formation in central Sichuan. Wang [41] also showed the relationship between the reflection coefficient of the HTI medium and the incident angle according to the Rüger formula. However, only when the incident angle is greater than 20° does the reflection coefficient change slightly. The incident angle that can be resolved by the three types of models established by us is less than 15° . However, there are also some disadvantages. For example, we only consider the fracture-cavity reservoir under study as an HTI medium, and there is still a lack of consideration for an anisotropy medium.

In this paper, together with analyzing the development of fracture density of three types of reservoirs in the Dengying Formation of the central Sichuan Basin, knowledge has been extended to a certain level. However, some limitations in practical application still exist; for instance, the reservoir cavities are not well understood in fine detail because of the limitations of research methods in the study of cavity characteristics. At the same time, we also found that the silicon content of the carbonate reservoir of Dengying Formation in the study area is abnormal, and the formation silicon content has a certain impact on the response characteristics of AVAZ forward modeling of fracture cave reservoir. Eliminating the influence of silicon will make the results more accurate, which needs to be improved. Therefore, we intend to perform physical rock modeling to further investigate the rock physical parameters of the cavity background and thus improve the accuracy of the seismic model. The reservoirs of the Dengying Formation could be developed by reference to the conclusions of forward modeling, which provides us with feasible and applicable evidence for future research on the seismic identification of reservoirs and prediction of fracture distribution in the Dengying Formation of central Sichuan.

5. Conclusions

Apart from the different reservoir types of Sinian Dengying Formation in the Gaoshiti block of central Sichuan were summarized, a better understanding of reservoir space was made to have an establishment of different reservoir geological models. By calculating various reservoir reflection coefficients with anisotropic HTI media to conduct AVAZ forward modeling, the analysis of multiple reservoirs' characteristics of the amplitude change and azimuth anisotropy was performed. Based on the results above, the following conclusions are obtained.

The top interface of the fracture-cavity reservoir presents a positive reflection on a whole. On the premise of the same incidence angle, the reflection coefficient of the fracture-cavity reservoir increases as fracture density raises, being symmetrical along the symmetrical axis of fracture. While the incidence angle marks higher, the reflection coefficient is in decline. Azimuth parallel to the normal direction of the fracture surface makes the reflection coefficient lowest, but when it parallels to fracture strike, the reflection coefficient turns to the highest.

Reservoir type, incidence angle, and azimuth change are considered the main impacts on seismic response characteristics of the fracture-cavity reservoir. The amplitude intensity is the most obvious in type III reservoir, while it remains the lowest in type II, and type I ranks as the second. The increase in incident angle brings about a gradual decline in amplitude. The amplitude reaches the highest when the azimuth is parallel to the normal direction of the fracture surface; however, it will come down to the lowest as the azimuth is perpendicular to the normal direction of the fracture surface. The fracture density fails to affect the amplitude when the azimuth angle is parallel to the direction of the fracture. However, When the azimuth is parallel to the normal direction of the fracture surface, the amplitude decreases with the increase in fracture density.

Author Contributions: Conceptualization, Y.L. and B.G.; methodology, Y.L. and B.G.; software, Z.Z. and J.J.; validation, Y.L.; formal analysis, Z.Z.; investigation, Y.L.; resources, Z.Z.; data curation, Y.L.; writing—original draft preparation, Y.L.; writing—review and editing, R.P.; supervision, R.P. All authors have read and agreed to the published version of the manuscript.

Funding: This research was funded by the National Nature Science Foundation of China under Grant No. (41804120), and three National Grand Project for Science and Technology of China, under Grant No. (2016ZX0561-001, 2016ZX05047-002 and 2016ZX05062-002).

Institutional Review Board Statement: Not applicable.

Informed Consent Statement: Not applicable.

Data Availability Statement: The datasets used in the current study are available from the corresponding author on reasonable request.

Conflicts of Interest: The authors declare no conflict of interest.

Nomenclature

AVAZ	Amplitude Variation with Azimuth
AVO	Amplitude variation with offset
HTI	Horizontal Transverse Isotropy
VTI	Vertical Transverse Isotropy
TTI	Tilted symmetry axis Transverse Isotropy
Type I	fracture-cavity reservoir + siliceous strip + fracture-cavity reservoir
Type II	fracture-cavity reservoir + siliceous strip + cave type reservoir
Type III	fracture-cavity reservoir + siliceous strip + relatively dense layer
P-P wave	Incident p-wave to receive p-wave

References

- Du, J.H.; Zou, C.N.; Xu, C.C.; He, H.; Shen, P.; Yang, Y. Theoretical and technical innovations in strategic discovery of a giant gas field in Cambrian Longwangmiao Formation of central Sichuan paleo-uplift, Sichuan Basin. *Pet. Explor. Dev.* **2014**, *41*, 268–277. [[CrossRef](#)]
- Yu, Z.R.; Yang, Y.; Xiao, Y.; He, B.; Song, L.; Zhang, M. High-yield well modes and production practices in the Longwangmiao Fm gas reservoirs, Anyue Gas Field, central Sichuan Basin. *Nat. Gas Ind.* **2016**, *36*, 69–79. (In Chinese) [[CrossRef](#)]
- Jiang, R.; Zhao, L.; Xu, A.; Ashraf, U.; Yin, J.; Song, H.; Anees, A. Sweet spots prediction through fracture genesis using multi-scale geological and geophysical data in the karst reservoirs of Cambrian Longwangmiao Carbonate Formation, Moxi-Gaoshiti area in Sichuan Basin, South China. *J. Pet. Explor. Prod. Technol.* **2022**, *12*, 1313–1328. [[CrossRef](#)]
- Ullah, J.; Luo, M.; Ashraf, U.; Pan, H.; Anees, A.; Li, D.; Ali, J. Evaluation of the geothermal parameters to decipher the thermal structure of the upper crust of the Longmenshan fault zone derived from borehole data. *Geothermics* **2020**, *98*, 102268. [[CrossRef](#)]

5. Ashraf, U.; Zhang, H.; Anees, A.; Nasir, M.H.; Ali, M.; Ullah, Z.; Zhang, X. Application of unconventional seismic attributes and unsupervised machine learning for the identification of fault and fracture network. *Appl. Sci.* **2020**, *10*, 3864. [[CrossRef](#)]
6. Ashraf, U.; Zhang, H.; Anees, A.; Ali, M.; Zhang, X.; Shakeel, A.S.; Nasir, M.H. Controls on reservoir heterogeneity of a shallow-marine reservoir in Sawan gas field, SE Pakistan: Implications for reservoir quality prediction using acoustic impedance inversion. *Water* **2020**, *12*, 2972. [[CrossRef](#)]
7. Ma, L.W.; Gu, H.M.; Li, Z.J.; Lv, S.S. Simulation of carbonate fracture-cavern reservoir reflection characteristics with forward modeling. *Oil Geophys. Prospect.* **2015**, *502*, 290–297. (In Chinese)
8. Sun, M.S.; Liu, C.Y.; Yang, Y.; Zhang, G.; Feng, C. The forward modeling of fracture and cave carbonate reservoirs of the Yingshan Formation in Tazhong area, Tarim Basin. *Earth Sci. Front.* **2017**, *24*, 339–349. (In Chinese)
9. Ma, L.W.; Yang, Q.Y.; Gu, H.M. Simulation of reservoir seismic response in the northern slope of the middle Tarim Basin with random fracture-cavern media model. *Oil Geophys. Prospect.* **2016**, *51*, 1119–1127+1049. (In Chinese)
10. Yang, P.; Sun, Z.D.; Li, H.Y. Key influence factors of Karst fracture-cave bodies on reflection characteristics. *Oil Geophys. Prospect.* **2015**, *50*, 523–529. (In Chinese)
11. Bachrach, B. Uncertainty and nonuniqueness in linearized AVAZ for orthorhombic media. *Lead. Edge* **2015**, *34*, 1048–1050, 1052, 1054, 1056. [[CrossRef](#)]
12. Wang, L.P.; Gu, H.M.; Li, Z.J. The characteristic analysis of AVO attribution for fractured-Vuggy reservoir model. *Geol. Sci. Technol. Inf.* **2011**, *32*, 197–201. (In Chinese)
13. Chen, J.; Zhang, H.; Wang, J.; Wang, H.; Chen, F.; Meng, X. Carbonate fracture-cave reservoir prediction with prestack AVO. *Pet. Geophys. Explor.* **2014**, *49*, 1191–1198.
14. Narhari, S.R.; Al-Qadeeri, B.; Dashti, Q. Application of prestack orthotropic AVAZ inversion for fracture characterization of a deep carbonate reservoir in northern Kuwait. *Lead. Edge* **2015**, *34*, 1488–1493. [[CrossRef](#)]
15. Liu, X.W.; Guo, Z.Q.; Liu, C. Anisotropy rock physics model for the Longmaxi shale gas reservoir, Sichuan Basin, China. *Appl. Geophys.* **2017**, *14*, 21–30. [[CrossRef](#)]
16. Lu, C.; Wang, X.; Lu, X.; Zhou, Q.; Zhang, Y.; Sun, Z.; Xiao, L.; Liu, X. Evaluation of Hydrocarbon Generation Using Structural and Thermal Modeling in the Thrust Belt of Kuqa Foreland Basin, NW China. *Geofluids* **2020**, *2020*, 8894030. [[CrossRef](#)]
17. Fu, X.B.; Yu, J.S.; Yuan, J.L. Modelling analysis of the limitation of P-wave AVAZ inversion. *J. Appl. Geophys.* **2019**, *170*, 103842. [[CrossRef](#)]
18. Wang, C.C.; Shi, Z.J.; Hu, X.Q.; Chen, H. Geophysical response and formation mechanism analysis of fractured-vuggy reservoir in Maokou formation in southeast Sichuan. *Prog. Geophys.* **2011**, *26*, 1683–1689. (In Chinese)
19. Xiao, F.S.; Chen, K.; Ran, Q.; Zhang, X.; Xie, B.; Liu, X.G. New understandings of the seismic modes of high productivity wells in the Sinian Dengying Fm gas reservoirs in the Gaoshiti area, Sichuan Basin. *Nat. Gas Ind.* **2018**, *38*, 8–15. (In Chinese) [[CrossRef](#)]
20. Weng, X.B.; Pan, R.F.; Luo, W.J.; Zhu, Z.P.; Jin, J.N. Petrophysical model for dolomite reservoirs: A case study in the fourth member of the Dengying formation at a platform margin in the Gaoshiti area, central Sichuan Basin. *Geophys. Prospect. Pet.* **2021**, *60*, 983–994.
21. Bao, J.; Cheng, G. Permeability measurement of the fracture-matrix system with 3D embedded discrete fracture model. *Pet. Sci.* **2022**, *in press*. [[CrossRef](#)]
22. Bao, J.; Chen, Z.; Xian, C. Investigations of CO₂ storage capacity and flow behavior in shale formation. *J. Pet. Sci. Eng.* **2022**, *208*, 109659.
23. Thai, B.N.; Vo Thanh, H.; Sugai, Y.; Sasaki, K.; Nguete, R.; Quang, T.P.H.; Bao, M.L.; Hai, N.L.N. Applying the hydrodynamic model to optimize the production for crystalline basement reservoir, X field, Cuu Long Basin, Vietnam. *J. Pet. Explor. Prod. Technol.* **2020**, *10*, 31–46. [[CrossRef](#)]
24. Thanh, H.V.; Sugai, Y.; Nguete, R.; Sasaki, K. Integrated workflow in 3D geological model construction for evaluation of CO₂ storage capacity of a fractured basement reservoir in Cuu Long Basin, Vietnam. *Int. J. Greenh. Gas Control* **2019**, *90*, 102826. [[CrossRef](#)]
25. Shu, M.C. The application of improved AVAZ method in predicting the fractured reservoir. *CT Theory Appl.* **2017**, *26*, 45–52.
26. Hou, K.; Li, L.; Luo, Z.; Yang, X.J.; Zhao, H.J.; Zhao, W.C. The research of seismic forward modeling method for the inhomogeneous fracture media. *Geophys. Geochem. Explor. Calc. Technol.* **2018**, *41*, 563–571.
27. Long, L.; Chen, K.; Peng, D.; Xu, X.; Zhao, A. Karst reservoir prediction method based on AVO characteristic analysis. In Proceedings of the SPG/SEG Nanjing 2020 International Geophysical Conference, Nanjing, China, 13–16 September 2020; pp. 750–752. (In Chinese).
28. Li, X.Z.; Guo, Z.H.; Wan, Y.J.; Liu, X.H.; Zhang, M.L.; Xie, W.R. Geological characteristics and development strategies for Cambrian Longwangmiao Formation gas reservoir in Anyue gas field, Sichuan Basin, SW China. *Pet. Explor. Dev.* **2017**, *44*, 398–406. [[CrossRef](#)]
29. Li, Z.Y.; Jiang, H.; Wang, Z.C.; Wang, T.S.; Nu, W.H.; Lv, Z.G. Control of tectonic movement on hydrocarbon accumulation in the Sinian strata, Sichuan Basin. *Nat. Gas Ind.* **2014**, *34*, 23–30. (In Chinese)
30. Wang, N.; Wei, G.Q.; Yang, W.; Wu, S.J. Different characters of palaeo-uplift and their control actions on natural gas accumulation in Sichuan Basin. *Reserv. Eval. Dev.* **2016**, *6*, 1–8. (In Chinese)
31. Gao, S.S.; Hu, Z.M.; Liu, H.X.; Ye, L.Y.; An, W.G. Microscopic pore characteristics of different lithological reservoirs. *Acta Pet. Sin.* **2016**, *37*, 248–256. (In Chinese)

32. Thomsen, L. Weak elastic anisotropy. *Geophysics* **1986**, *51*, 1954–1966. [[CrossRef](#)]
33. Thomsen, L. Elastic anisotropy due to aligned cracks in porous rock. *Geophys. Prospect.* **1995**, *43*, 805–829. [[CrossRef](#)]
34. Wang, X.; Zhang, F.; Li, S. The Architectural Surfaces Characteristics of Sandy Braided River Reservoirs, Case Study in Gudong Oil Field, China. *Geofluids* **2021**, *2021*, 8821711. [[CrossRef](#)]
35. Wang, X.; Liu, Y.; Hou, J. The relationship between synsedimentary fault activity and reservoir quality—A case study of the Ek1 formation in the Wang Guantun area, China. *Interpretation* **2020**, *8*, 15–24. [[CrossRef](#)]
36. Wang, X.; Zhou, X.; Li, S. Mechanism Study of Hydrocarbon Differential Distribution Controlled by the Activity of Growing Faults in Faulted Basins: Case Study of Paleogene in the Wang Guantun Area, Bohai Bay Basin, China. *Lithosphere* **2021**, *2021*, 7115985. [[CrossRef](#)]
37. Li, H.D.; Dong, S.H.; Zhao, X.C.; Lu, L.; Zhang, C.; Li, S.J. Numerical simulation with staggered grid high-order difference method for porosity and Thomsen anisotropic coefficients of gas coal. *Geophys. Geochem. Explor.* **2011**, *35*, 855–859. (In Chinese)
38. Tsvankin, I. P-wave signatures and notation for transversely isotropic media. an overview. *Geophysics* **1996**, *61*, 467–483. [[CrossRef](#)]
39. Bakulin, A.; Grechka, V.; Tsvankin, I. Estimation of fracture parameters from reflection seismic data—Part I. HTI model due to a single fracture set. *Geophysics* **2000**, *65*, 1788–1802. [[CrossRef](#)]
40. Rüger, A. P-wave reflection coefficients for transversely isotropic models with vertical and horizontal axis of symmetry. *Geophysics* **1997**, *62*, 713–722. [[CrossRef](#)]
41. Wang, T.; Yuan, S.; Shi, P.; Shuai, D.; Luo, C.; Wang, S. AVAZ inversion for fracture weakness based on three-term Rüger equation. *J. Appl. Geophys.* **2019**, *162*, 184–193. [[CrossRef](#)]